J. Fluid Mech. (2007), *vol.* 593, *pp.* 235–254.
doi:10.1017/S002211200700866X Printed in the United Kingdom

Contour dynamics in complex domains

DARREN CROWDY[1] AND AMIT SURANA[2]

[1]Department of Mathematics, Massachusetts Institute of Technology 2-384, 77 Massachusetts Avenue, Cambridge, MA 02139, USA

[2]Department of Mechanical Engineering, Massachusetts Institute of Technology 3-335, 77 Massachusetts Avenue, Cambridge, MA 02139, USA

(Received 26 September 2006 and in revised form 18 August 2007)

This paper demonstrates that there is a contour dynamics formulation for the evolution of uniform vortex patches in any finitely connected planar domain bounded by impenetrable walls. A general numerical scheme is presented based on this formulation. The algorithm makes use of conformal mappings and follows the evolution of a conformal pre-image of a given vortex patch in a canonical multiply connected circular pre-image region. The evolution of vortex patches can be computed given just the conformal map from this pre-image region to the physical fluid region. The efficacy of the scheme is demonstrated by illustrative examples.

1. Introduction

A common model for the dynamics of vorticity in planar flows is the point-vortex model (Newton 2001; Saffman 1992). These models, in which a vorticity distribution is modelled by a collection of δ-functions, are useful for reducing the dimensionality of the governing Euler equations to a set of nonlinear ordinary differential equations and can provide accurate predictions for the gross behaviour of the centres of vorticity. By their very nature they fail, however, to resolve any detailed geometrical structure of the vortex regions, or to capture any finite-area dynamical effects such as vortex merger or vortex breakup.

A better model of vorticity that has proved, over the last few decades, to be of enduring value is the vortex-patch model (Saffman 1992). A vortex patch is a finite-area region of uniform vorticity. These models are capable of capturing the finite-area effects that are precluded by the point-vortex model and, importantly, do not involve a total sacrifice of the reduction in dimensionality of the original problem. This is because the evolution of a uniform vortex region only requires the tracking of its boundary since an initially uniform vortex region remains uniform as it evolves. Based on this crucial observation, Zabusky, Hughes & Roberts (1979) introduced the numerical scheme now commonly known as contour dynamics. It has since been enhanced, notably by Dritschel (1988*a*), to incorporate a contour surgery procedure whereby long-time integrations can be performed that deal effectively with the formation of thin extended vortical filaments. A review of contour dynamics methods has been presented by Pullin (1992).

Compared with studies of the dynamics of vorticity in unbounded regions, the literature on vortex motion in regions bounded by impenetrable walls is limited. This problem is, however, of classical interest and has commanded the attention of (among others) Kirchhoff (see Lamb 1932) and Routh (1881). There is now a systematic theory for computing the evolution of a collection of point vortices in

a simply connected region. This theory rests on it being a Hamiltonian dynamical system, the governing Hamiltonian being referred to as the Kirchhoff–Routh path function (Saffman 1992). Lin (1941*a*, *b*) later showed that this Hamiltonian structure survives when the fluid domain is multiply connected and deduced the existence of a generalized Kirchhoff–Routh path function. Lin's theory is, however, non-constructive. In a constructive theory which marries Lin's results with elements of classical function theory, Crowdy & Marshall (2005*a*) have devised a general method for computing the motion of point vortices in complex multiply connected geometries.

One study which adapts a contour dynamics algorithm for computations of patch motion involving impenetrable walls has been performed by Pullin (1981). Motivated by applications to geophysical fluid dynamics, Johnson & McDonald (2005*a*, *c*) have contributed a series of works in which the motion of both point vortices and vortex patches in regions bounded by impenetrable walls is studied. For example, in Johnson & McDonald (2005*a*, *c*), the problem of vortex motion near a wall containing gaps is considered. In their numerical simulations of vortex patch motion near gaps in walls, Johnson & McDonald make use of the following idea. If an infinite straight wall has no gap, the motion of a vortex patch above this wall can be computed using a regular free-space contour dynamics algorithm by replacing the wall with a 'reflected patch' (i.e. the vortex patch reflected in the infinite straight wall) and then computing the two-patch evolution of this reflectionally symmetric configuration. When gaps are present, these authors continue to use a free-space contour dynamics calculation together with an 'image' vortex patch, but they add what amounts to a 'background flow contribution' which corrects for the gaps in the wall. This ingenious approach provides a method for computing the vortex-patch evolution, but it is specific to the particular geometry under investigation there.

Jomaa & Macaskill (2005) have considered similar problems to those addressed in this paper, but from a different perspective. They do not use a pure contour dynamics approach, but employ a hybrid method involving an underlying grid to gain efficiency over contour dynamics methods for complex flows. Other related work, based on similar ideas, is due to Macaskill, Padden & Dritschel (2003) who focus on flows in a cylinder.

Similar efforts to devise formulations of contour dynamics involving boundaries have been made by those interested in the motion of non-neutral plasmas in Malmberg–Penning traps. The equations of motion for such plasmas are isomorphic to the Euler equations for an ideal incompressible fluid. Backhaus, Fajans & Wurtele (1988) and Coppa, Peano & Peinetti (2002) have considered a formulation of contour dynamics in a circular cylinder. Their approach, which relies on ideas from the method of images (which they call an 'image-charge' method), has many features in common with those devised by Johnson & McDonald (2005*b*, *c*). Again, however, these methods are limited in that they are relevant only to vortex motion involving circular boundaries.

This paper presents a flexible contour dynamics method for computing the motion of vortex patches in complex multiply connected geometries. The key idea is to consider a conformal map to the physical region of interest from a conformally equivalent circular pre-image region. Given this conformal map, the evolution of the pre-image of a given vortex patch is calculated. This calculation is facilitated by knowledge of the explicit functional form of the relevant Green's function in this pre-image region (see Crowdy & Marshall 2005*a*). Moreover, while the instantaneous boundary-value problem for finding the velocity field generated by a finite-area vortex

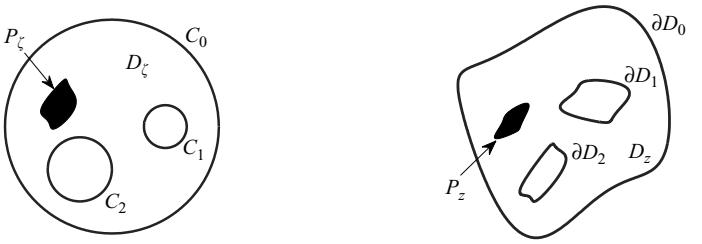

FIGURE 1. The idea of the algorithm: a conformal map $z(\zeta)$ transplants a circular pre-image domain D_ζ to the physical fluid region D_z containing a vortex patch P_z. The pre-image of P_z in D_ζ is P_ζ.

patch is not conformally invariant, it turns out that, by appropriate manipulations of the governing equations, a contour dynamics formulation can still be found.

The advantage of this algorithm is that it can be applied, in principle, to any multiply connected fluid region for which a conformal mapping from a circular pre-image region can be found, either analytically or numerically. It can be combined with existing numerical conformal mapping codes to compute the motion of vortex patches in more or less arbitrary flow domains.

2. Mathematical formulation

Let D_z be an arbitrary multiply connected region of fluid with finite connectivity. For the moment, it will be assumed that D_z is a bounded domain. Let $M \geqslant 0$ be an integer and let $\{D_j | j = 1, \ldots, M\}$ denote M 'islands' inside D_z and let the boundary of D_j be ∂D_j. The outer boundary enclosing the islands will be ∂D_0. All the boundaries of the fluid region are taken to be impenetrable barriers to the flow. It is known, from an extension of the Riemann mapping theorem (Goluzin 1969), that D_z is conformally equivalent to some circular pre-image region D_ζ consisting of the unit ζ-disk with M smaller circular disks excised. Let C_0 denote the unit circle in a parametric ζ-plane and let $\{C_j | j = 1, \ldots, M\}$ be the circular boundaries of the enclosed disks. Let $q_j \in \mathbb{R}$ and $\delta_j \in \mathbb{C}$, respectively, denote the radius and centre of the circle C_j. The domain D_z itself will dictate what these parameters are (they are the conformal moduli (Nehari 1982) of the domain D_z). Let $z(\zeta)$ be the conformal mapping from D_ζ to D_z. We assume that $z(\zeta)$ is a known function, given either as an analytical formula or computable by some numerical conformal mapping algorithm. Everything deduced below also holds when the mapping $z(\zeta)$ has a simple pole in D_ζ so that the image is an unbounded fluid domain. Suppose that the fluid inside D_z is irrotational except for a time-evolving uniform vortex patch P_z. Let the boundary of the vortex patch be ∂P_z. Let P_ζ be the pre-image region in D_ζ corresponding to the patch P_z in D_z. The image of the boundary ∂P_ζ of P_ζ under the mapping $z(\zeta)$ is precisely the boundary ∂P_z of P_z. Figure 1 shows the notation. It is important to emphasize that we will not solve for the actual motion of a vortex patch in the pre-image domain D_ζ. Our aim is to demonstrate the general result that there always exists a contour dynamics formulation for this problem. That is, the computation of the velocities of the patch boundary in the physical domain D_z can always be reduced to the evaluation of a contour integral. Our approach is constructive.

Let $G(z, z_\alpha)$ be the Green's function in D_z, the Laplacian of which has a δ-function singularity at some point z_α inside D_z so that

$$\nabla^2 G(z, z_\alpha) = -\delta(z - z_\alpha), \tag{2.1}$$

with G taking a constant value on all the boundaries of D_z. In particular, on the outer boundary ∂D_0, it can be assumed, without loss of generality, that

$$G = 0 \text{ on } \partial D_0. \tag{2.2}$$

$G(z, z_\alpha)$ will also satisfy the conditions that the circulations around all the enclosed islands are zero, i.e.

$$\oint_{\partial D_j} \frac{\partial G}{\partial n} \mathrm{d}s = 0, \qquad j = 1, \ldots, M. \tag{2.3}$$

In fact, G is the special Green's function considered by Lin (1941*a*) in his studies of point-vortex motion in multiply connected domains; the same function was later dubbed the 'hydrodynamic Green's function' by Flucher & Gustafsson (1997) (see also Flucher 1999).

Let ψ be the streamfunction associated with the flow in D_z generated by the patch P_z. It satisfies the same boundary conditions, and zero circulation conditions, as the Green's function just introduced. Finally, let the uniform vorticity inside P_z be ω_0 so that

$$\nabla^2 \psi = \begin{cases} -\omega_0, & z \in P_z, \\ 0, & z \notin P_z. \end{cases} \tag{2.4}$$

By Green's identity and the divergence theorem,

$$\begin{aligned} \int\int_{D_z} (\psi \nabla^2 G - G \nabla^2 \psi) \mathrm{d}A_z &= \int\int_{D_z} \nabla \cdot (\psi \nabla G - G \nabla \psi) \, \mathrm{d}A_z \\ &= \oint_{\partial D_z} \left(\psi \frac{\partial G}{\partial n} - G \frac{\partial \psi}{\partial n} \right) \mathrm{d}s, \end{aligned} \tag{2.5}$$

where $\mathrm{d}A_z$ denotes the area element in D_z. The line integrals on the right-hand side can all be shown to vanish owing to the boundary conditions that both ψ and G are constant on ∂D_z (and vanish on ∂D_0) together with the conditions of zero circulation around all the interior islands. It follows that

$$\psi(z, \bar{z}) = \int\int_{P_z} \omega_0 \; G(z, z_\alpha) \, \mathrm{d}A_{z_\alpha}, \tag{2.6}$$

where we have used (2.4), and where the integration is an area integral with respect to the z_α variable.

The boundary-value problem satisfied by the Green's function G is a conformally invariant one. It therefore follows that

$$G(z, z_\alpha) = G_0(\zeta, \alpha), \tag{2.7}$$

where $z_\alpha = z(\alpha)$ and where $G_0(\zeta, \alpha)$ is the Green's function whose explicit form was found by Crowdy & Marshall (2005*a*). It is

$$G_0(\zeta, \alpha) = -\frac{1}{2\pi} \log \left| \frac{\omega(\zeta, \alpha)}{\alpha \omega(\zeta, \overline{\alpha}^{-1})} \right|, \tag{2.8}$$

where $\omega(\zeta, \alpha)$ is the so-called Schottky–Klein prime function (see Crowdy & Marshall 2005*a*) associated with the domain D_ζ. Equation (2.8) can also be written

$$G_0(\zeta, \alpha) = -\frac{1}{4\pi} \log \left(\frac{\omega(\zeta, \alpha) \overline{\omega}(\overline{\zeta}, \overline{\alpha})}{|\alpha|^2 \omega(\zeta, \overline{\alpha}^{-1}) \overline{\omega}(\overline{\zeta}, \alpha^{-1})} \right). \tag{2.9}$$

The particular functional form of $G_0(\zeta, \alpha)$, as given in (2.8) or (2.9), will be crucial in what follows.

On using (2.7) and (2.9) in (2.6), we obtain

$$\psi(z, \bar{z}) = \int\int_{P_z} \omega_0 \; G(z, z_\alpha)\, \mathrm{d}A_{z_\alpha}$$
$$= -\frac{\omega_0}{4\pi} \int\int_{P_\zeta} \log\left(\frac{\omega(\zeta, \alpha)\overline{\omega}(\overline{\zeta}, \overline{\alpha})}{|\alpha|^2 \omega(\zeta, \overline{\alpha}^{-1})\overline{\omega}(\overline{\zeta}, \alpha^{-1})}\right) \frac{\mathrm{d}z(\alpha)}{\mathrm{d}\alpha} \overline{\left(\frac{dz(\alpha)}{d\alpha}\right)}\, \mathrm{d}A_\alpha, \quad (2.10)$$

where $\mathrm{d}A_\alpha$ denotes the area element with respect to the variable α and we have introduced the usual Jacobian scaling $\mathrm{d}A_{z_\alpha} = |\mathrm{d}z/\mathrm{d}\alpha|^2 \mathrm{d}A_\alpha$.

Now, the complex velocity $u - \mathrm{i}v$ in the z-plane (which will be required in order to update the patch boundary) is given by

$$u - \mathrm{i}v = 2\mathrm{i}\frac{\partial \psi}{\partial z}\bigg|_{\bar{z}} = 2\mathrm{i}\frac{\partial \Psi}{\partial \zeta}\bigg|_{\bar{\zeta}} \frac{1}{z_\zeta(\zeta)}, \quad (2.11)$$

where

$$\Psi(\zeta, \bar{\zeta}) \equiv \psi(z(\zeta), \overline{z(\zeta)}), \quad (2.12)$$

and where $z_\zeta(\zeta)$ denotes the derivative with respect to ζ. However, on differentiating (2.10) with respect to ζ, we obtain

$$\frac{\partial \Psi}{\partial \zeta}\bigg|_{\bar{\zeta}} = -\frac{\omega_0}{4\pi} \int\int_{P_\zeta} \left(\frac{\omega_\zeta(\zeta, \alpha)}{\omega(\zeta, \alpha)} - \frac{\omega_\zeta(\zeta, \bar{\alpha}^{-1})}{\omega(\zeta, \bar{\alpha}^{-1})}\right) \frac{\mathrm{d}z(\alpha)}{\mathrm{d}\alpha} \overline{\left(\frac{\mathrm{d}z(\alpha)}{\mathrm{d}\alpha}\right)} \mathrm{d}A_\alpha, \quad (2.13)$$

where $\omega_\zeta(\zeta, \alpha)$ denotes the derivative of $\omega(\zeta, \alpha)$ with respect to its first argument ζ. This can be written as

$$\frac{\partial \Psi}{\partial \zeta}\bigg|_{\bar{\zeta}} = -\frac{\omega_0}{4\pi} \int\int_{P_\zeta} \left(\frac{\omega_\zeta(\zeta, \alpha)}{\omega(\zeta, \alpha)} \frac{\mathrm{d}z(\alpha)}{\mathrm{d}\alpha} \overline{\left(\frac{\mathrm{d}z(\alpha)}{\mathrm{d}\alpha}\right)}\right) \frac{\mathrm{d}\alpha \wedge \mathrm{d}\overline{\alpha}}{2\mathrm{i}}$$
$$+ \frac{\omega_0}{4\pi} \int\int_{P_\zeta} \left(\frac{\omega_\zeta(\zeta, \bar{\alpha}^{-1})}{\omega(\zeta, \bar{\alpha}^{-1})} \frac{\mathrm{d}z(\alpha)}{\mathrm{d}\alpha} \overline{\left(\frac{\mathrm{d}z(\alpha)}{\mathrm{d}\alpha}\right)}\right) \frac{\mathrm{d}\alpha \wedge \mathrm{d}\overline{\alpha}}{2\mathrm{i}}, \quad (2.14)$$

where we have introduced the notation (see Ablowitz & Fokas 1995)

$$\mathrm{d}A_\alpha = \frac{\mathrm{d}\alpha \wedge \mathrm{d}\overline{\alpha}}{2\mathrm{i}}. \quad (2.15)$$

This can further be rewritten in the more suggestive form

$$\frac{\partial \Psi}{\partial \zeta}\bigg|_{\bar{\zeta}} = -\frac{\omega_0}{8\pi\mathrm{i}} \int\int_{P_\zeta} \frac{\partial}{\partial \bar{\alpha}} \left(\frac{\omega_\zeta(\zeta, \alpha)}{\omega(\zeta, \alpha)} \overline{z(\alpha)} \frac{\mathrm{d}z(\alpha)}{\mathrm{d}\alpha}\right) \mathrm{d}\alpha \wedge \mathrm{d}\overline{\alpha}$$
$$+ \frac{\omega_0}{8\pi\mathrm{i}} \int\int_{P_\zeta} \frac{\partial}{\partial \alpha} \left(\frac{\omega_\zeta(\zeta, \bar{\alpha}^{-1})}{\omega(\zeta, \bar{\alpha}^{-1})} z(\alpha) \overline{\left(\frac{\mathrm{d}z(\alpha)}{\mathrm{d}\alpha}\right)}\right) \mathrm{d}\alpha \wedge \mathrm{d}\overline{\alpha}. \quad (2.16)$$

The complex version of Green's theorem takes two different forms and both of these will now be useful. First, given any function Φ regular everywhere in some region D,

$$\int\int_D \frac{\partial \Phi}{\partial \bar{z}} \mathrm{d}z \wedge \mathrm{d}\bar{z} = \oint_{\partial D} \Phi \, \mathrm{d}z, \quad (2.17)$$

where ∂D is the boundary of D. Another form is

$$-\int\int_D \frac{\partial \Phi}{\partial z} \mathrm{d}z \wedge \mathrm{d}\bar{z} = \oint_{\partial D} \Phi \mathrm{d}\bar{z}. \tag{2.18}$$

If ζ is inside D_ζ, but outside the vortex patch P_ζ, then all the integrands in (2.16) are regular functions for α (and $\bar{\alpha}$) inside P_ζ. It follows, since both (2.17) and (2.18) can then be used in (2.16), that

$$\left.\frac{\partial \Psi}{\partial \zeta}\right|_{\bar{\zeta}} = -\frac{\omega_0}{8\pi \mathrm{i}} \oint_{\partial P_\zeta} \left(\frac{\omega_\zeta(\zeta,\alpha)}{\omega(\zeta,\alpha)} \overline{z(\alpha)} \frac{\mathrm{d}z(\alpha)}{\mathrm{d}\alpha} \right) \mathrm{d}\alpha$$
$$-\frac{\omega_0}{8\pi \mathrm{i}} \oint_{\partial P_\zeta} \left(\frac{\omega_\zeta(\zeta,\bar{\alpha}^{-1})}{\omega(\zeta,\bar{\alpha}^{-1})} z(\alpha) \overline{\left(\frac{\mathrm{d}z(\alpha)}{\mathrm{d}\alpha} \right)} \right) \mathrm{d}\bar{\alpha}. \tag{2.19}$$

The integrands in these line integrals are all known functions. Equation (2.19) is important: it shows that the calculation of the velocity field outside the patch has been reduced to the evaluation of a line integral. In particular, as ζ tends to a point on ∂P_ζ (so that z tends to a point on the physical patch boundary ∂P_z), by taking principal part integrals in (2.19) and using (2.11), we can readily compute the velocity of the patch boundary ∂P_z in the physical plane. This is all that is required to update the patch shape. Once the updated patch P_z is found, the updated pre-image patch P_ζ can also be found. What we have demonstrated is that there is a contour dynamics formulation for the evolution of a vortex patch in any finitely connected domain bounded by impenetrable walls.

A feature of vortex dynamics in multiply connected domains (which is not a concern in the simply connected case) is the condition that the round-island circulations must be constant in time. This dynamical constraint is a requirement imposed by Kelvin's circulation theorem (see Saffman 1992). It is significant that the formulae derived above automatically enforce the constancy of the round-island circulations. It is therefore not necessary to impose explicitly any additional conditions to enforce these integral constraints.

In summary, up to conformal mapping (i.e. knowledge of $z(\zeta)$), the above formulation is completely general and shows that vortex-patch motion in any multiply connected region admits a contour dynamics formulation.

3. Numerical implementation

The vortex patch P_z induces a velocity field

$$u - \mathrm{i}v = 2\mathrm{i} \left.\frac{\partial \psi}{\partial z}\right|_{\bar{z}} = \frac{2\mathrm{i}}{z_\zeta(\zeta)} \left.\frac{\partial \Psi}{\partial \zeta}\right|_{\bar{\zeta}}, \tag{3.1}$$

where $\partial \Psi / \partial \zeta$ is given by (2.19). Equation (3.1) is valid for any point $\zeta \in D_\zeta$ outside the vortex patch P_ζ and hence gives the velocity induced by the patch outside the patch.

The Schottky–Klein prime function described in Crowdy & Marshall (2005*a*) can be defined by an infinite product

$$\omega(\zeta,\gamma) = (\zeta - \gamma)\hat{\omega}(\zeta,\gamma), \tag{3.2}$$

where

$$\hat{\omega}(\zeta,\gamma)=\prod_{\theta_i\in\Theta''}\frac{(\theta_i(\zeta)-\gamma)(\theta_i(\gamma)-\zeta)}{(\theta_i(\zeta)-\zeta)(\theta_i(\gamma)-\gamma)} \tag{3.3}$$

and

$$\theta_i(\zeta)=\delta_i+\frac{q_i^2\zeta}{1-\overline{\delta}_i\zeta}. \tag{3.4}$$

Recall that $q_i\in\mathbb{R}$ and $\delta_i\in\mathbb{C}$ are, respectively, the radius and centre of the circle C_j. Θ'' is an appropriate subset of the Schottky group (see Crowdy & Marshall (2005*a*) for details). First note that

$$\frac{\omega_\zeta(\zeta,\alpha)}{\omega(\zeta,\alpha)}=\frac{1}{\zeta-\alpha}+\frac{\hat{\omega}_\zeta(\zeta,\alpha)}{\hat{\omega}(\zeta,\alpha)}, \tag{3.5}$$

where the second term on the right-hand side, which is the modification to the free-space contribution deriving from the presence of the walls, is regular everywhere in D_ζ. Therefore, for any point $\zeta\in D_\zeta\backslash P_\zeta$, we see that

$$\left.\frac{\partial\Psi}{\partial\zeta}\right|_{\overline{\zeta}}=I_r(\zeta)+I_s(\zeta), \tag{3.6}$$

where

$$I_r(\zeta)=-\frac{\omega_0}{8\pi\mathrm{i}}\left[\oint_{\partial P_\zeta}\frac{z(\alpha)\overline{z}_\zeta(\overline{\alpha})}{(\zeta-\overline{\alpha}^{-1})}\,\mathrm{d}\overline{\alpha}+\oint_{\partial P_\zeta}\left(\frac{\hat{\omega}_\zeta(\zeta,\alpha)}{\hat{\omega}(\zeta,\alpha)}z_\zeta(\alpha)\overline{z}(\overline{\alpha})\right)\mathrm{d}\alpha\right.$$
$$\left.+\oint_{\partial P_\zeta}\left(\frac{\hat{\omega}_\zeta(\zeta,\overline{\alpha}^{-1})}{\hat{\omega}(\zeta,\overline{\alpha}^{-1})}z(\alpha)\overline{z}_\zeta(\overline{\alpha})\right)\mathrm{d}\overline{\alpha}\right] \tag{3.7}$$

and

$$I_s(\zeta)=\frac{\omega_0}{8\pi\mathrm{i}}\oint_{\partial P_\zeta}\frac{z_\zeta(\alpha)\overline{z}(\overline{\alpha})}{\alpha-\zeta}\mathrm{d}\alpha. \tag{3.8}$$

The above decomposition shows that the vortex patch evolves with a velocity field which has two contributions: $I_r(\zeta)$ is the velocity induced by the image vorticity distribution while $I_s(\zeta)$ is the self-induced velocity contribution. $I_r(\zeta)$ is regular everywhere in D_ζ, but the integrand of $I_s(\zeta)$ becomes singular as ζ approaches a point on the patch boundary ∂P_ζ. We examine how to evaluate these integrals in § 3.2.

In a numerical implementation of contour dynamics, three main issues arise (see Pullin (1992) for a general discussion): (*a*) accurate representation of the patch boundary ∂P_ζ at each time step; (*b*) accurate computation of the contour integrals appearing in (3.6); (*c*) advection of the contour. In the following subsections, we discuss each of these points separately.

3.1. *Contour representation*

Each contour ∂P_z and ∂P_ζ will be represented by a distribution of nodes with interpolating functions used to approximate the contour between nodes. We will use a node-adjustment algorithm to maintain acceptable accuracy as the lengths of the vortex boundaries become extended, or highly curved, during a simulation. At this point, we have a choice as to the domain in which we perform the advection of the vortex patch contour and the adjustment of the node distribution to maintain accuracy: we can either update the pre-image contour ∂P_ζ or the physical contour ∂P_z. We have investigated both choices numerically and have found that updating

the position of the physical contour ∂P_z is more accurate. To do so, however, still requires knowledge of the pre-image patch P_ζ since it is in the ζ-plane that the patch boundary velocities are computed. One reason we suspect it is preferable to update P_z (rather than P_ζ) is that conformal mappings are angle-preserving maps, but they do not preserve lengths or areas. During a typical simulation, the area and perimeter of P_ζ can both vary greatly (although its area is always bounded above since P_ζ is confined to the unit disk). In the physical domain, however, the patch area is conserved (even though the perimeter can still vary dramatically owing to filamentation effects).

A second advantage of advecting the contour ∂P_z, and dynamically adjusting the nodes thereon, is that this feature already exists in contour dynamics codes and has been well studied. The new ingredient of our approach is the use of a pre-image conformal mapping plane to compute the boundary velocities of the vortex patch when geometrically complex boundaries are involved.

Following Dritschel (1988*a*), to represent the contour ∂P_z we employ a locally determined cubic polynomial as the interpolation function. With this scheme, the contour between two nodes j and $j+1$ on ∂P_z, for example, is given by

$$\tilde{\beta}_j(s) = z_j + s(z_{j+1} - z_j) + \mathrm{i}\tilde{\eta}_j(s)(z_{j+1} - z_j), \tag{3.9}$$

where

$$\tilde{\eta}_j(s) = \tilde{\alpha}_j s + \tilde{\beta}_j s^2 + \tilde{\gamma}_j s^3, \tag{3.10}$$

for $0 \leqslant s \leqslant 1$. The coefficients in $\tilde{\eta}(s)$ are

$$\tilde{\alpha}_j = -\tfrac{1}{3}e_j\kappa_j - \tfrac{1}{6}e_j\kappa_{j+1}, \quad \tilde{\beta}_j = \tfrac{1}{2}e_j\kappa_j, \quad \tilde{\gamma}_j = \tfrac{1}{6}e_j(\kappa_{j+1} - \kappa_j), \tag{3.11}$$

where, $e_j = |z_{j+1} - z_j|$ and κ_j is the curvature at node j computed by passing a circle through the nodes labelled $j-1$, j and $j+1$. The redistribution of nodes is controlled by a node density function ρ whose contour integral with respect to arclength gives the total number of nodes on a given contour. Our node adjustment is controlled by the same parameters δ, μ, L and a introduced by Dritschel (1988*a*) and discussed in detail there. δ is a problem-dependent distance which serves as a small-scale cutoff for resolving the contour. μ controls the overall density of nodes. L is taken to be a typical length scale of large-scale vorticity distribution in the problem and $a \in (0, 1)$ controls how quickly the node density rises with the curvature. In all the cases considered in this paper, the initial vortex patch is taken to be circular with radius R with $\omega_0 = 2\pi$. We have then chosen the parameter values $L = R$, $\delta = 10^{-4}$, $a = 2/3$ and $\mu \sim \pi/10 - \pi/30$.

Once a suitable distribution of nodes on ∂P_z has been found, these nodes are transplanted, via the known conformal mapping, to ∂P_ζ and a (different) set of interpolants is then found there. For example, we use

$$\beta_j(s) = \zeta_j + s(\zeta_{j+1} - \zeta_j) + \mathrm{i}\eta_j(s)(\zeta_{j+1} - \zeta_j), \tag{3.12}$$

with the same prescription for finding $\eta_j(s)$ as described above for $\tilde{\eta}_j(s)$. It was generally found that a well-resolved contour ∂P_z leads, after conformal mapping of nodes, to a well-resolved contour ∂P_ζ.

3.2. *Computation of contour integrals*

The success of current contour dynamics algorithms rests, in part, on the fact that the singular contribution to the relevant integrals can be performed analytically,

leaving only a regular integral to be computed numerically. At first sight, the above formulation involving (essentially arbitrary) conformal mapping functions in the integrands seems to jeopardize the prospect of evaluating the singular integrals in a numerically stable fashion. However, we will now show how to overcome this difficulty.

With the representation of the contour given in the previous section, (3.7) becomes

$$\begin{aligned} I_r(\zeta) = &- \frac{\omega_0}{8\pi \mathrm{i}} \sum_{j=1}^{N} \int_0^1 \frac{z(\beta_j(s))\overline{z}_\zeta(\overline{\beta}_j(s))}{(\zeta - \overline{\beta_j(s)}^{-1})} \overline{\beta}_j'(s)\,\mathrm{d}s \\ &- \frac{\omega_0}{8\pi \mathrm{i}} \sum_{j=1}^{N} \int_0^1 \left(\frac{\hat{\omega}_\zeta(\zeta, \beta_j(s))}{\hat{\omega}(\zeta, \beta_j(s))} z_\zeta(\beta_j(s))\overline{z}(\overline{\beta}_j(s)) \right) \beta_j'(s)\,\mathrm{d}s \\ &- \frac{\omega_0}{8\pi \mathrm{i}} \sum_{j=1}^{N} \int_0^1 \left(\frac{\hat{\omega}_\zeta(\zeta, \overline{\beta}_j^{-1}(s))}{\hat{\omega}(\zeta, \overline{\beta}_j^{-1}(s))} z(\beta_j(s))\overline{z}_\zeta(\overline{\beta}_j(s)) \right) \overline{\beta}_j'(s)\,\mathrm{d}s, \end{aligned} \tag{3.13}$$

where N denotes the number of nodal points on the curve and where primes denote differentiation with respect to s. Since, at a nodal point $\zeta = \zeta_k$, the integrals appearing in I_r remain regular, $I_r(\zeta_k)$ can be computed using standard numerical integrators.

The computation of I_s, however, requires greater care. The first step is to desingularize this integral. It is a consequence of Cauchy's theorem that, for ζ outside the patch,

$$\frac{\omega_0}{8\pi \mathrm{i}} \oint_{\partial P_\zeta} \frac{\mathrm{d}\alpha}{\alpha - \zeta} = 0. \tag{3.14}$$

Adding a multiple of this to I_s does not change the latter so we can write

$$I_s(\zeta) = \frac{\omega_0}{8\pi \mathrm{i}} \oint_{\partial P_\zeta} \left(\frac{\overline{z}(\overline{\alpha})z_\zeta(\alpha) - \overline{z}(\overline{\zeta})z_\zeta(\zeta)}{\alpha - \zeta} \right) \mathrm{d}\alpha, \tag{3.15}$$

which can now be expressed as

$$I_s(\zeta) = \frac{\omega_0}{8\pi \mathrm{i}} \sum_{j=1}^{N} \int_0^1 \left(\frac{z_\zeta(\beta_j(s))\overline{z}(\overline{\beta}_j(s)) - \overline{z}(\overline{\zeta})z_\zeta(\zeta)}{\beta_j(s) - \zeta} \right) \beta_j'(s)\,\mathrm{d}s. \tag{3.16}$$

To compute $I_s(\zeta_k)$ at a nodal point ζ_k we split the above sum as

$$\begin{aligned} I_s(\zeta_k) = &\frac{\omega_0}{8\pi \mathrm{i}} \sum_{\substack{j=1 \\ j \neq k-1,k}}^{N} \int_0^1 \left(\frac{z_\zeta(\beta_j(s))\overline{z}(\overline{\beta}_j(s)) - \overline{z}(\overline{\zeta_k})z_\zeta(\zeta_k)}{\beta_j(s) - \zeta_k} \right) \beta_j'(s)\,\mathrm{d}s \\ &+ \frac{\omega_0}{8\pi \mathrm{i}} \sum_{j=k-1,k} \int_0^1 \left(\frac{z_\zeta(\beta_j(s))\overline{z}(\overline{\beta}_j(s)) - \overline{z}(\overline{\zeta_k})z_\zeta(\zeta_k)}{\beta_j(s) - \zeta_k} \right) \beta_j'(s)\,\mathrm{d}s. \end{aligned} \tag{3.17}$$

The first sum in (3.17) is the non-local contribution to the velocity field at ζ_k. Since each term in the sum is regular, the non-local contribution can be computed in the same way as $I_r(\zeta_k)$. The second sum corresponds to the local contribution to the velocity at node ζ_k and can be approximated analytically as follows. Since the segment $\beta_j(s)$ for $j = k-1,\ k$ of the contour lies in the vicinity of ζ_k, Taylor expansion of the

numerator in the integrand about ζ_k yields, up to first order, for $j = k-1, k$,

$$\frac{\omega_0}{8\pi \mathrm{i}} \int_0^1 \frac{1}{\beta_j(s) - \zeta_k} \left((\beta_j(s) - \zeta_k)\overline{z}(\overline{\zeta}_k) z_{\zeta\zeta}(\zeta_k) + (\overline{\beta}_j(s) - \overline{\zeta}_k))|z_\zeta(\zeta_k)|^2 + \cdots \right) \beta_j'(s)\,\mathrm{d}s$$
$$= \frac{\omega_0}{8\pi \mathrm{i}} \left[\overline{z}(\overline{\zeta}_k) z_{\zeta\zeta}(\zeta_k) \int_0^1 \beta_j'(s)\,\mathrm{d}s + |z_\zeta(\zeta_k)|^2 \int_0^1 \frac{\overline{\beta}_j(s) - \overline{\zeta}_k}{\beta_j(s) - \zeta_k} \beta_j'(s)\,\mathrm{d}s + \cdots \right]. \quad (3.18)$$

Using the cubic representation (3.9) for $\beta_j(s)$ in (3.18), the contribution corresponding to $j = k$ in the second sum of (3.17) becomes

$$\frac{\omega_0}{8\pi \mathrm{i}} \overline{z}(\overline{\zeta}_k) z_{\zeta\zeta}(\zeta_k)(\zeta_{k+1} - \zeta_k) \int_0^1 (1 + \mathrm{i}\eta_k'(s))\,\mathrm{d}s$$
$$+ \frac{\omega_0}{8\pi \mathrm{i}} |z_\zeta(\zeta_k)|^2 (\overline{\zeta}_{k+1} - \overline{\zeta}_k) \int_0^1 \frac{(s - \mathrm{i}\eta_k(s))}{(s + \mathrm{i}\eta_k(s))} (1 + \mathrm{i}\eta_k'(s))\,\mathrm{d}s + \cdots \quad (3.19)$$

Since $\eta_k(1) = \alpha_k + \beta_k + \gamma_k = 0$, we have

$$\int_0^1 (1 + \mathrm{i}\eta_k'(s))\,\mathrm{d}s = 1, \quad \int_0^1 \frac{(s - \mathrm{i}\eta_k(s))}{(s + \mathrm{i}\eta_k(s))} (1 + \mathrm{i}\eta_k'(s))\,\mathrm{d}s = 1 - \mathscr{I}_k, \quad (3.20)$$

with

$$\mathscr{I}_k = 2 \int_0^1 \log(1 + \mathrm{i}[\alpha_k + \beta_k s + \gamma_k s^2])\,\mathrm{d}s, \quad (3.21)$$

and the integral can be approximated by

$$\frac{\omega_0}{8\pi \mathrm{i}} [\overline{z}(\overline{\zeta}_k) z_{\zeta\zeta}(\zeta_k)(\zeta_{k+1} - \zeta_k) + |z_\zeta(\zeta_k)|^2 (\overline{\zeta}_{k+1} - \overline{\zeta}_k)(1 - \mathscr{I}_k)]. \quad (3.22)$$

Following similar steps for $j = k-1$, we obtain the contribution

$$\frac{\omega_0}{8\pi \mathrm{i}} [\overline{z}(\overline{\zeta}_k) z_{\zeta\zeta}(\zeta_k)(\zeta_k - \zeta_{k-1}) + |z_\zeta(\zeta_k)|^2 (\overline{\zeta}_k - \overline{\zeta}_{k-1})(1 - \mathscr{I}_{k-1})], \quad (3.23)$$

where

$$\mathscr{I}_{k-1} = 2 \int_0^1 \log(1 - \mathrm{i}\alpha_{k-1} s + \mathrm{i}\gamma_{k-1} s^2)\,\mathrm{d}s. \quad (3.24)$$

The integrals $\mathscr{I}_{k-1}$ and $\mathscr{I}_k$ can be computed analytically (e.g. by a change of variable and use of reduction formulae), but we omit the details.

3.3. *Advection of the contour*

The patch boundary ∂P_z position is updated by advecting each node $\{z_k | k = 1, \ldots, N\}$. By (3.1), the evolution of z_k satisfies the complex ordinary differential equation

$$\frac{\mathrm{d}\overline{z}_k}{\mathrm{d}t} = \frac{2\mathrm{i}}{z_\zeta(\zeta_k)} \frac{\partial \Psi}{\partial \zeta}\bigg|_{\overline{\zeta}} (\zeta_k, \overline{\zeta}_k). \quad (3.25)$$

Once the position $z_k(t)$ has been updated, the corresponding pre-image point $\zeta_k(t)$ satisfying $z_k(t) = z(\zeta_k(t))$ can be found.

In the calculations to follow, we use an explicit fourth-order Runge–Kutta scheme for the integration of the governing ordinary differential equations. The time step Δt used in this scheme has to be chosen appropriately, especially if, during the evolution, the patch P_ζ becomes close to the boundaries of the circles $\{C_j | j = 0, 1, \ldots, M\}$ in D_ζ. The time step Δt used in the Runge–Kutta scheme varies in the range 0.01–0.05.

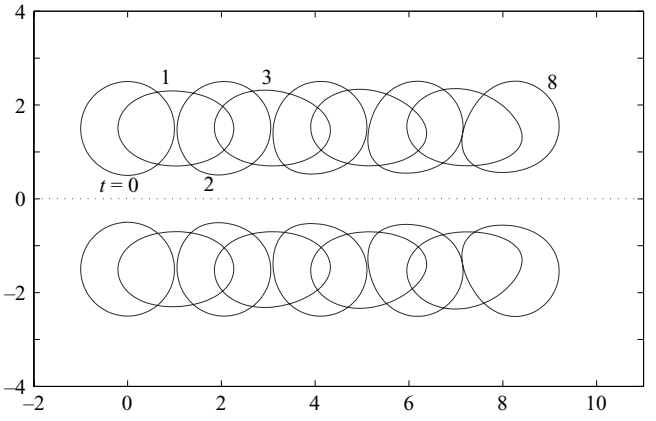

FIGURE 2. Evolution of two initially circular patches, of area π, with centres separated by distance 3, computed by a free-space contour dynamics code.

Numerical integration is carried out using Simpson's rule. Any derivatives (of analytic functions) are computed using two-sided finite differencing whenever they cannot be obtained analytically.

Despite many points of similarity, it is important to note that our algorithm differs from that described by Dritschel (1988*a*). First, we do not here perform any contour surgery (see Dritschel 1988*a* for details). Secondly, the numerical evaluation of the integrals just presented does not share the same high degree of accuracy as that devised by Dritschel (1988*a*). For these two reasons, we do not expect our current numerical implementation of the algorithm to be able to perform integrations over very long times. However, it can still be used to ascertain the viability of our new approach.

4. Numerical examples

4.1. *Motion of a patch near a wall*

Our first calculation provides a validation of the new method. We consider the motion of a single vortex patch near an infinite straight wall. In this case, the same dynamical evolution of the patch can be obtained by removing the wall and considering the motion of two vortex patches in an unbounded fluid region, the second patch being the reflection in the (now absent) wall of the first patch and having vorticity of opposite sign. This allows us to directly compare a calculation performed using the new algorithm with a two-vortex calculation performed using existing free-space contour dynamics codes. Here, we employ the contour surgery code due to Dritschel (1988*a*). Figure 2 shows the calculation up to $t = 8$ (where we have rescaled time with respect to 2π) of an initially circular vortex patch at a height 1.5 above the wall. For comparison, figure 3 shows the same calculation performed using the new method. It gives excellent agreement with the calculation in figure 2. Figure 4 shows a second calculation, performed using Dritschel's contour surgery code, for an initially circular vortex patch with centre at a height 1.05 above the wall. Now, the onset of filamentation effects is apparent. Figure 5 shows the same calculation performed using the new method and corroborates the fact that it is capable of capturing such filamentation effects. With careful study, minor differences in the lengths of the

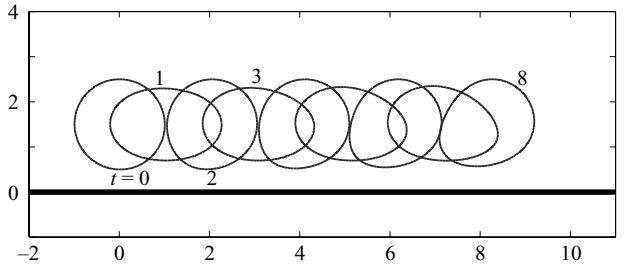

FIGURE 3. Evolution of a single circular patch, of area π, at height 1.5 above an infinite straight wall. This calculation uses the new method.

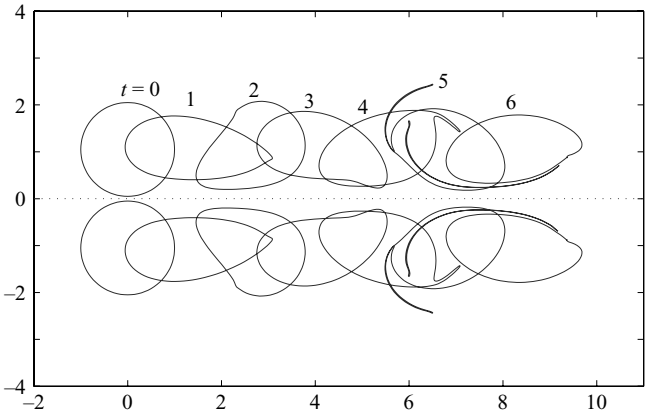

FIGURE 4. Evolution of two initially circular patches, of area π, with centres separated by distance 2.1, as computed by a (free-space) contour dynamics code.

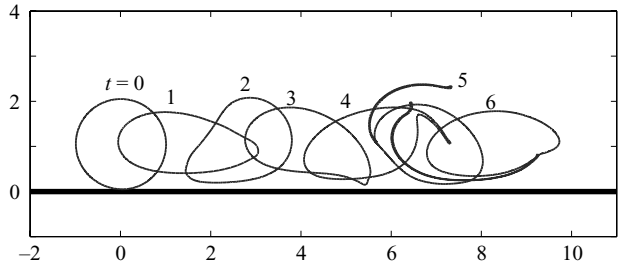

FIGURE 5. Evolution of a single circular patch, of area π, at height 1.05 above an infinite straight wall. This calculation uses the new method.

more extended filaments can be observed. However, the velocity integrals in the new formulation are not calculated to the same high degree of accuracy as in Dritschel's code, so such differences must be expected using our current implementation.

4.2. *Motion of a patch near a gap in a wall*

Further validation of our scheme is afforded by the problem of vortex-patch motion near a gap in a wall. There has been much recent interest in such problems. Johnson & McDonald (2005*b*) consider the case of a single gap and have computed the evolution

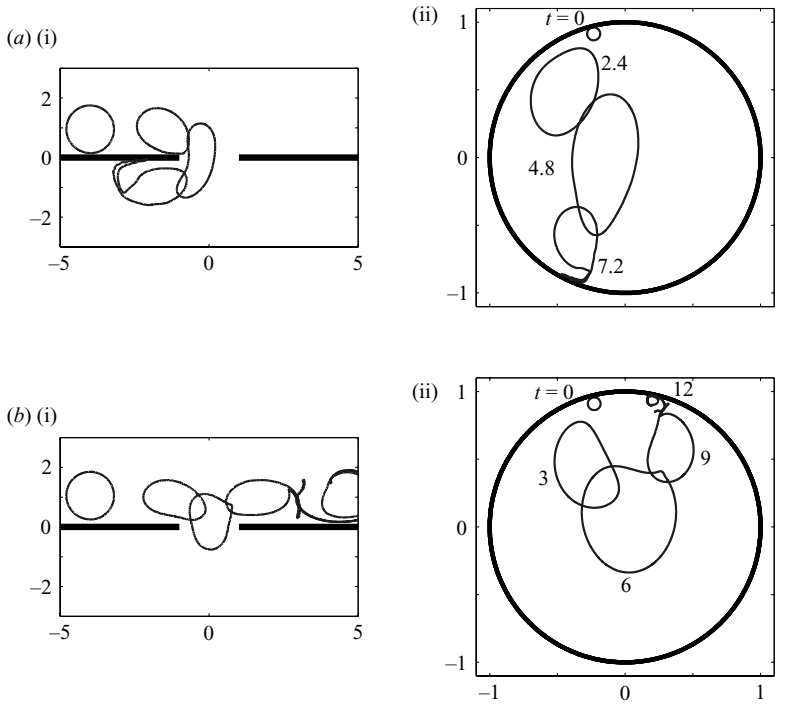

FIGURE 6. Evolution of an initially circular vortex patch of radius 0.8, vorticity 2π, initially (*a*) at $(-4, 0.95)$ and (*b*) at $(-4, 1.05)$. The corresponding evolution in the unit ζ-disk is shown in (*a*)(ii) and (*b*)(ii). These figures compare well to figures 7 and 8 of Johnson & McDonald (2005*b*).

of a point vortex (analytically) and of a vortex patch (numerically). Later, they extended the investigation to the case of multiple gaps and gave explicit details of the two-gap case (see Johnson & McDonald 2005*c*). An analytical treatment of the motion of point vortices in the general multiple-gap case has been given by Crowdy & Marshall (2006). They combine the generalized Kirchhoff–Routh theory described in Crowdy & Marshall (2005*a*) with analytical forms for the conformal mappings taking multiply connected circular pre-image domains D_ζ to fluid regions involving barriers with multiple gaps. The required conformal map in the single-gap case is

$$z(\zeta) = \frac{L\zeta}{(1+\zeta^2)}. \tag{4.1}$$

This takes the interior of the unit ζ-disk to the exterior of an infinite straight wall, along the real axis, with a symmetric gap of width L centred at the origin. Figure 6 shows the simulation results. In figure 6(*a*)(i) the initial centroid location and patch radius are the same as considered figure 7 of Johnson & McDonald (2005*b*). The initial location $(-4, 0.95)$ puts the patch below the critical separatrix trajectory for a point vortex to pass through the gap and, indeed, the vortex patch also passes through the gap. The evolution of this patch in the pre-image ζ-plane is also featured in figure 6. This highlights the point made earlier on how much the area and perimeter of the pre-image patch can vary during a typical simulation. Figure 6(*b*) is a second simulation where the initial starting location of the patch is further from the wall (at a distance of 1.05) than the critical-point vortex trajectory and the vortex patch leaps

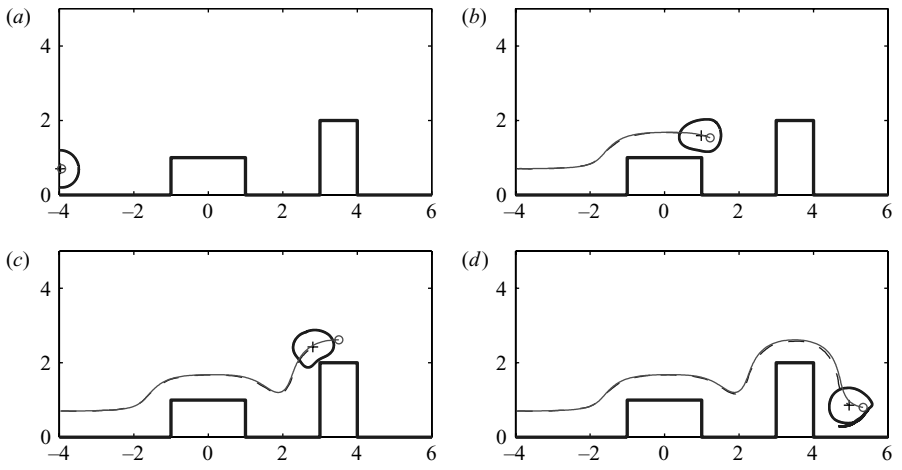

FIGURE 7. Motion of an initially circular vortex patch, of vorticity 2π with initial radius 0.5, over topography. The conformal mapping here is provided by the SC Toolbox of Driscoll. Times shown are $t = 0.05, 10, 17.5, 23$.

across the gap, just as a point vortex would. This figure compares well with figure 8 of Johnson & McDonald (2005*b*) and displays only minor differences in the lengths of the filaments (which we again attribute to a cumulative effect associated with differences in the accuracy of the velocity integral evaluations in the two simulations). The corresponding evolution in the pre-image ζ-plane for this case is also shown.

4.3. *Motion of a patch near topography*

Equation (4.1) is a special case of a Schwarz–Christoffel map (see Ablowitz & Fokas 1995). A strength of our method is its immediate applicability, with only minor modifications, to any region for which a conformal map from a circular pre-image region is available. To show this, we have combined our generalized contour dynamics algorithm with a Matlab code called the SC toolbox,† which computes the parameters in a general Schwarz–Christoffel mapping from a unit ζ-disk to any target simply connected polygonal region as described in Driscoll & Trefethen (2002). In figure 7, the evolution of a vortex patch travelling past an infinite straight wall with two polygonal protrusions is shown. By the final frame, a small filamentary thread of vorticity is seen to develop, as might be expected given the high shear rates it experiences owing to its proximity to the wall (cf. figure 5). In figure 7, we have also superposed the trajectory of a point vortex of the same circulation (drawn dashed) to highlight the fact that the vortex-patch trajectory follows it very closely despite the large shape deformations of the patch induced by the presence of the wall.

4.4. *Electron vortices in plasma traps*

Mitchell, Wang & Rossi (2006) have studied the evolution of elliptical electron vortices in Malmberg–Penning traps. Such traps are hollow conducting cylinders in which a uniform magnetic field acts on clouds of electrons. Under the relevant approximations, the motion of such electron clouds in these traps is governed by an equation that is isomorphic to the two-dimensional Euler equations, the electron density playing the analogous role to vorticity. Mitchell *et al.* (2006) have studied how the stability of

† T. Driscoll, SC Toolbox, www.math.udel.edu/driscoll/SC.

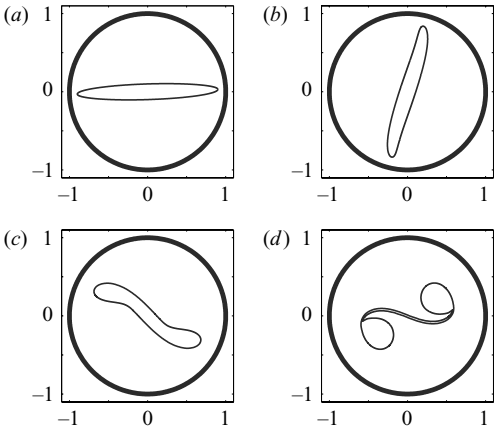

FIGURE 8. Evolution of an elliptical vortex patch, of vorticity 2π, with $a = 0.9$ and $a/b = 9$. The trap is a circle with unit radius. Times shown are (*a*) $t = 0.05$, (*b*) 2.0, (*c*) 4.0, (*d*) 6.0.

elliptical electron vortices is affected both by the presence of the walls of the trap and a 'smoothed out' vorticity profile at the vortex boundary (i.e. they do not model the vortices as vortex patches with sharp edges).

Our method can perform numerical simulations of electron clouds, modelled as patches with sharp edges, in traps of various cross-sections. Backhaus *et al.* (1988) and Coppa *et al.* (2002) have also been concerned with a formulation of contour dynamics in a trap of circular cross-section. Figure 8 shows the evolution of an elliptical vortex patch with aspect ratio $a/b = 9$ computed using the new technique (note that the conformal map here is just the identity map). The patch develops instability and ultimately saturates into a configuration of two circular orbiting vortices. This computation is in qualitative agreement with the experimental observations of Mitchell *et al.* (2006).

To further illustrate the flexibility of our method, we present some results for the case of a square trap. Again, we make use of the SC Toolbox to provide the required conformal map from the unit ζ-disk to the square trap even though this map can actually be found analytically in terms of elliptic functions (see Ablowitz & Fokas 1995).

Figures 9–11 show simulations of an initial elliptical vortex patch evolving in a square trap with sides of unit length. The semi-axes of the initial elliptical patch are denoted a and b. Its vorticity is taken to be 2π. The major semi-axis value of $a = 0.4$ is taken in all cases and the aspect ratio b/a gradually increased. Some interesting effects are observed. All initial elliptical vortices are linearly unstable, if they existed in free space, according to the stability calculations of Love (1983). Note that we do not seed our calculations with any initial perturbation of a chosen type, as in the circular trap simulations given in Mitchell *et al.* (2006); rather, it is a combination of the interaction of the vortex with the walls and the accumulation of small numerical inaccuracies which provide the seed for unstable modes to grow.

Figure 9 presents the case $a/b = 5$ and shows that the ellipse is unstable to the formation of two near-symmetric filamentary threads of vorticity emanating from the ends of the major axis of the ellipse. Since our numerical scheme does not incorporate any contour surgery effects, we are forced to terminate the simulation at $t = 8.3$. On the other hand, when $a/b = 7$ as in figure 11, the patch is unstable to the formation of

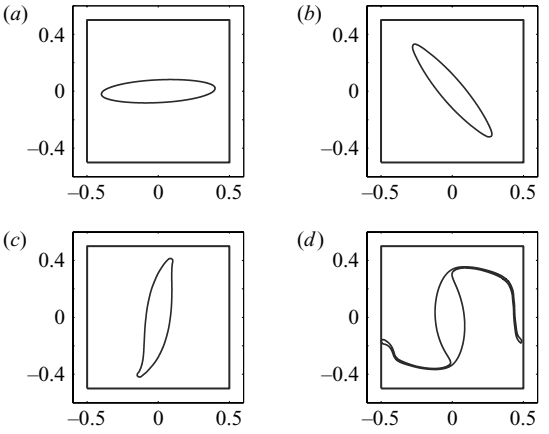

FIGURE 9. Evolution of an elliptical vortex patch, of vorticity 2π, with $a = 0.4$ and $a/b = 5$. The trap is square with sides of unit length. Times shown are (*a*) $t = 0.05$, (*b*) 2.5, (*c*) 5.0, (*d*) 8.3.

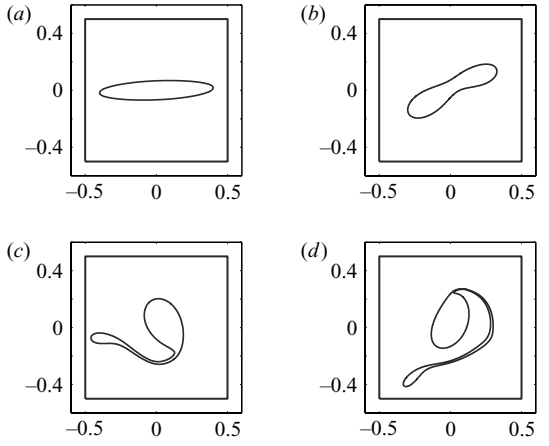

FIGURE 10. Evolution of an elliptical vortex patch, of vorticity 2π, with $a = 0.4$ and $a/b = 6$. The trap is square with sides of unit length. Times shown are (*a*) $t = 0.05$, (*b*) 8.3, (*c*) 12.5, (*d*) 14.0.

two well-defined and near-symmetrical vortex patches joined by a single filamentary thread. The final state appears to be a stable configuration of two co-rotating vortices. Figure 10 shows an intermediate case when $a/b = 6$. Figure 10(*b*) (which is reminiscent of figure 11*c*) suggests that the fate of the vortex will be to disintegrate into two co-rotating vortices as in figure 11; instead, however, the vortex develops into an asymmetric state consisting of a single coherent vortex ejecting a single filamentary thread.

4.5. *Multiply connected domains*

In all the examples given so far, the domains have been simply connected and the Schottky–Klein prime function was merely $\omega(\zeta, \gamma) = (\zeta - \gamma)$. It is important to demonstrate that our method applies to any finitely connected domain. The only modification is that the Schottky–Klein prime function must change to incorporate the topological differences associated with higher connected domains.

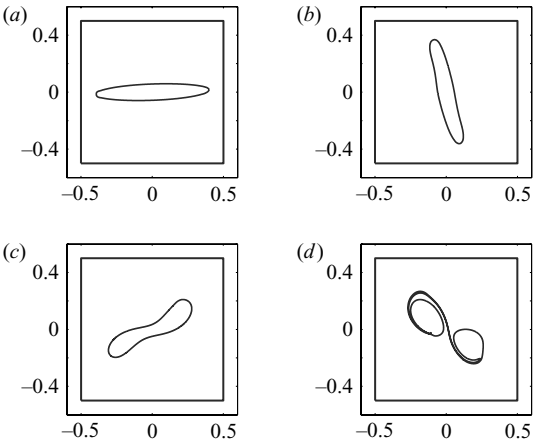

FIGURE 11. Evolution of an elliptical vortex patch, of vorticity 2π, with $a = 0.4$ and $a/b = 7$. The trap is square with sides of unit length. Times shown are (*a*) $t = 0.05$, (*b*) 2.5, (*c*) 5, (*d*) 8.25.

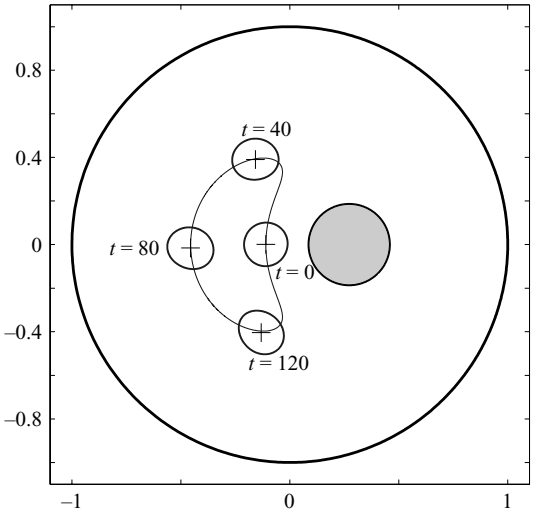

FIGURE 12. Evolution of a vortex patch in a doubly connected domain. The trajectory of a point vortex of equal circulation, calculated using the theory in Crowdy & Marshall (2005*a*), is superposed for comparison.

The evaluation of the Schottky–Klein prime functions involves the truncation of the infinite product (3.3). In practice, the products can be truncated in a natural way by including all mappings up to a certain level (Crowdy & Marshall 2005*a*). The computations which follow employ a level-three truncation (that is, all Möbius maps up to level 3 are included in the product – see Crowdy & Marshall (2005*a*) for further discussion). Experience shows that this can generally be expected to give 5–6 digits of accuracy in the evaluation of the prime function.

In Crowdy & Marshall (2005*a*), the authors present a general Kirchhoff–Routh theory applicable to the motion of point vortices in arbitrary multiply connected circular domains. The method here can be used to study the motion of vortex patches in the same class of domains. Figure 12 shows a typical calculation of a single

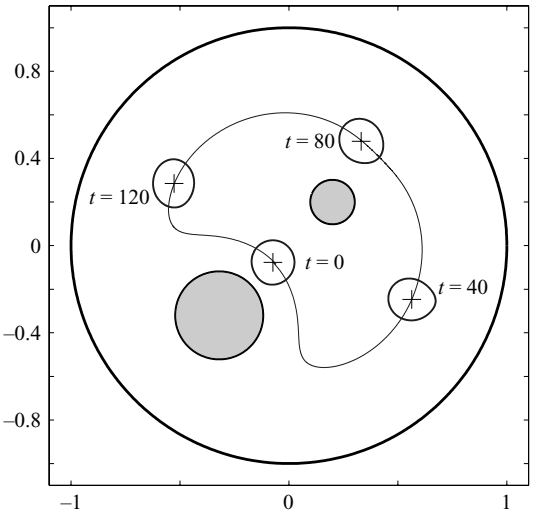

FIGURE 13. Evolution of a vortex patch in a triply connected domain. The trajectory of a point vortex of equal circulation, calculated using the theory in Crowdy & Marshall (2005*a*), is superposed for comparison.

vortex patch in a doubly connected domain consisting of a circular chamber with a single circular obstacle. For comparison, we have also superposed the trajectory for a point vortex, computed using the theory in Crowdy & Marshall (2005*a*), of equivalent circulation placed at the centroid of the initial patch. It is clear that the point-vortex and vortex-patch trajectories are very close. Finally, figure 13 shows a similar calculation when there are now two circular obstacles in the chamber so that the domain is triply connected. It should be clear that calculations in domains of any finite connectivity are similarly possible with no additional difficulty. For geometrically interesting domains, conformal mappings from multiply connected circular pre-image regions are required. For example, Crowdy & Marshall (2006) have given explicit formulae (actually, in terms of the Schottky–Klein prime function) for such conformal mappings to multiply connected slit domains and these can be used in combination with the present algorithm to study the dynamics of vortex patches through gaps in walls, a topic considered by Johnson & McDonald (2005*c*) with geophysical applications in mind.

5. Discussion

This paper has shown that the problem of vortex-patch evolution in any multiply connected domain has a contour dynamics formulation. By considering the evolution of a vortex patch in a circular multiply connected pre-image domain and by making use of conformal mappings from such canonical domains, a flexible numerical algorithm has been devised. Now, changes in geometry and topology of the domain simply involve changing the conformal mapping function and/or the Schottky–Klein prime function appearing in the general formulation.

The numerical implementation we have devised so far is not optimal; it is a basic code written simply to examine the viability of the proposed numerical scheme. Based on these preliminary calculations, we believe it is worth developing an enhanced algorithm. For example, the current algorithm does not perform any numerical

contour surgery (Dritschel 1988*a*). It should also be possible to evaluate the contour integrals (in the pre-image plane) giving the patch boundary velocity to a higher degree of accuracy. Further, to evaluate the Schottky–Klein prime function, we have here made use of an infinite product (3.3). For certain domains D_ζ, this infinite product is not convergent (or, even if convergent, it can converge very slowly). Nevertheless, the prime function is still a well-defined function in any circular domain D_ζ. Indeed, Crowdy & Marshall (2007) have devised an efficient numerical method for its evaluation. Since the latter algorithm works for broad classes of domains D_ζ, it is sensible to incorporate its use to evaluate the prime function for the purposes discussed in this paper.

A possible generalization of this work is to vortex-patch motion on the surface of a sphere with impenetrable boundaries. The problem of point-vortex motion on the surface of a sphere has been considered by Kidambi & Newton (2000) using a method of images approach and reappraised by Crowdy (2006) who shows how to apply conformal mapping theory to this problem. A contour surgery procedure on a spherical shell has been given by Dritschel (1988*b*). By combining all these ideas, the extension of the present algorithm to yield a flexible method of computing vortex-patch motion on a spherical shell with boundaries is feasible.

D. C. thanks the Leverhulme Trust for the award of a 2004 Philip Leverhulme Prize in Mathematics, the Engineering and Physical Sciences Research Council of the UK for an Advanced Research Fellowship and the European Science Foundation MISGAM project for partial support. He also acknowledges the hospitality of the Department of Mathematics at MIT where he performed this research as a visiting professor.

REFERENCES

Ablowitz, M. & Fokas, A. S. 1995 *Complex Variables*. Cambridge University Press.

Backhaus, E. Y., Fajans, J. & Wurtele, J. S. 1998 Application of contour dynamics to systems with cylindrical boundaries. *J. Comput. Phys.* **145**, 462–468.

Coppa, G. G. M., Peano, F. & Peinetti, F. 2002 Image-charge method for contour dynamics in systems with cylindrical boundaries. *J. Comput. Phys.* **182**, 392–417.

Crowdy, D. G. 2006 Point vortex motion of the surface of a sphere with impenetrable boundaries. *Phys. Fluids* **18**, 036602.

Crowdy, D. G. & Marshall, J. S. 2005*a* Analytical formulae for the Kirchoff–Routh path function in multiply connected domains. *Proc. R. Soc.* **461**, 2477–2501.

Crowdy, D. G. & Marshall, J. S. 2005*b* The motion of a point vortex around multiple circular islands. *Phys. Fluids* **17**, 056602.

Crowdy, D. G. & Marshall, J. S. 2006 The motion of a point vortex through gaps in walls. *J. Fluid Mech.* **551**, 31–48.

Crowdy, D. G. & Marshall, J. S. 2007 Computing the Schottky–Klein prime function on the Schottky double of planar domains. *Comput. Meth. Func. Theory* **7**(1), 293–308.

Driscoll, T. & Trefethen, L. N. 2002 *Schwarz–Christoffel Mappings*. Cambridge University Press.

Dritschel, D. G. 1988*a* Contour surgery: a topological reconnection scheme for extended integrations using contour dynamics. *J. Comput. Phys.* **77**, 240–266.

Dritschel, D. G. 1988*b* Contour dynamics/surgery on the sphere. *J. Comput. Phys.* **79**, 477.

Flucher, M. 1999 *Variational Problems with Concentration*. Birkhauser.

Flucher, M. & Gustafsson, B. 1997 Vortex motion in two dimensional hydrodynamics. *TRITA-MAT-1997-MA 02*, Stockholm, Royal Institute of Technology.

Goluzin, G. M. 1969 *Geometric Theory of Functions of a Complex Variable*. Translations of Mathematical Monographs, **26**, American Mathematical Society.

Johnson, E. R. & McDonald, N. R. 2005*a* The motion of a vortex near two circular cylinders. *Proc. R. Soc. Lond.* A **460**, 939–954.

Johnson, E. R. & McDonald, N. R. 2005*b* The motion of a vortex near a gap in a wall. *Phys. Fluids* **16**(2), 462.

Johnson, E. R. & McDonald, N. R. 2005*c* Vortices near barriers with multiple gaps. *J. Fluid Mech.* **531**, 335–358.

Jomaa, Z. & Macaskill, C. 2005 The embedded finite-difference method for the Poisson equation in a domain with an irregular boundary and Dirichlet boundary conditions. *J. Comput. Phys.* **202**, 488–506.

Kidambi, R. & Newton, P. K. 2000 Point vortex motion on a sphere with solid boundaries. *Phys. Fluids* **12**, 581.

Lamb, H. 1932 *Hydrodynamics.* Cambridge University Press.

Lin, C. C. 1941*a* On the motion of vortices in two dimensions. I: Existence of the Kirchhoff–Routh function. *Proc. Natl Acad. Sci.* **27**, 570–575.

Lin, C. C. 1941*b* On the motion of vortices in two dimensions. II: Some further investigations of the Kirchhoff–Routh function. *Proc. Natl Acad. Sci.* **27**, 575–577.

Love, A. E. H. 1983 On the stability of certain vortex motions. *Proc. Lond/ Math. Soc.* **25**, 18–42.

Macaskill, C. Padden, W. E. P. & Dritschel, D. G. 2003 The CASL algorithm for quasi-geostrophic flow in a cylinder. *J. Comput. Phys.* **188**, 232–251.

Mitchell, T. B. Wang, X. J. & Rossi, L. F. 2006 Stability of elliptical electron vortices. In *Non-neutral Plasma Physics VI, Workshop on Non-neutral Plasmas* (ed M. Drewsen, U. Uggerhoj & H. Knudsen).

Nehari, Z. 1982 *Conformal Mapping.* Dover.

Newton, P. K. 2001 *The N-Vortex Problem.* Springer.

Pozrikidis, C. 1997 *Introduction to Theoretical and Computational Fluid Dynamics.* Cambridge University Press.

Pullin, D. I. 1981 The nonlinear behaviour of a constant vorticity layer at a wall. *J. Fluid Mech*, **108**, 401.

Pullin, D. I. 1992 Contour dynamics methods *Annu. Rev. Fluid Mech.* **24**, 89–115.

Routh, E. J. 1881 Some applications of conjugate functions. *Proc. Lond. Math. Soc.* **12**, 73–89.

Saffman, P. G. 1992 *Vortex Dynamics.* Cambridge University Press.

Zabusky, N. J., Hughes, M. H. & Roberts, K. V. 1979 Contour dynamics for the Euler equations in two dimensions. *J. Comput. Phys.* **30**, 96.